



# INTERNATIONAL INSTALLATIONS



**EMIRATES PALACE,  
UNITED ARAB EMIRATES**



**AGUA CALIENTE CASINO,  
PALM SPRINGS, USA**



**THE CENTER BUILDING,  
HONGKONG**



**PRIDE SOUTH SEAS,  
SOUTH AFRICAN WATERS**



**SAMSUNG HOSPITAL,  
KOREA**



**PENINSULA HOTEL,  
TOKYO, JAPAN**

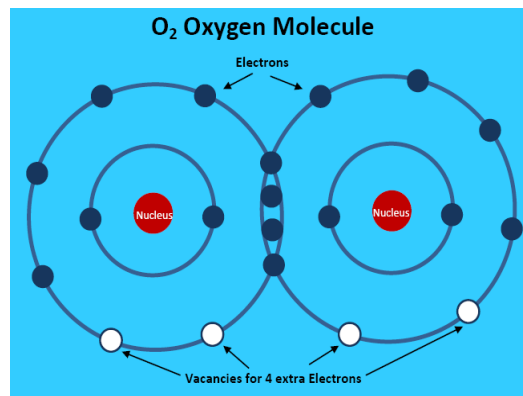
# THE 'BIO-OXYGEN' PROCESS

BIO-OXYGEN - The Natural Process © Copyright Bio-Oxygen 200711

## OXYGEN IS 'PARAMAGNETIC'

Oxygen is the only Gas in the Elemental Table that is "Paramagnetic". No other gas is paramagnetic. Being paramagnetic gives oxygen molecules the unique ability to absorb up to 4 extra electrons in the outer electron shell. When Oxygen Molecules gain 1-4 extra electrons they become 'magnetic' and agglomerate into Clusters. As an analogy, an electro magnet is just a lump of steel and is not magnetic and it only becomes a Magnet when the power is turned on and electrons begin to flow through the electro magnet. Oxygen behaves similar to an electro magnet.

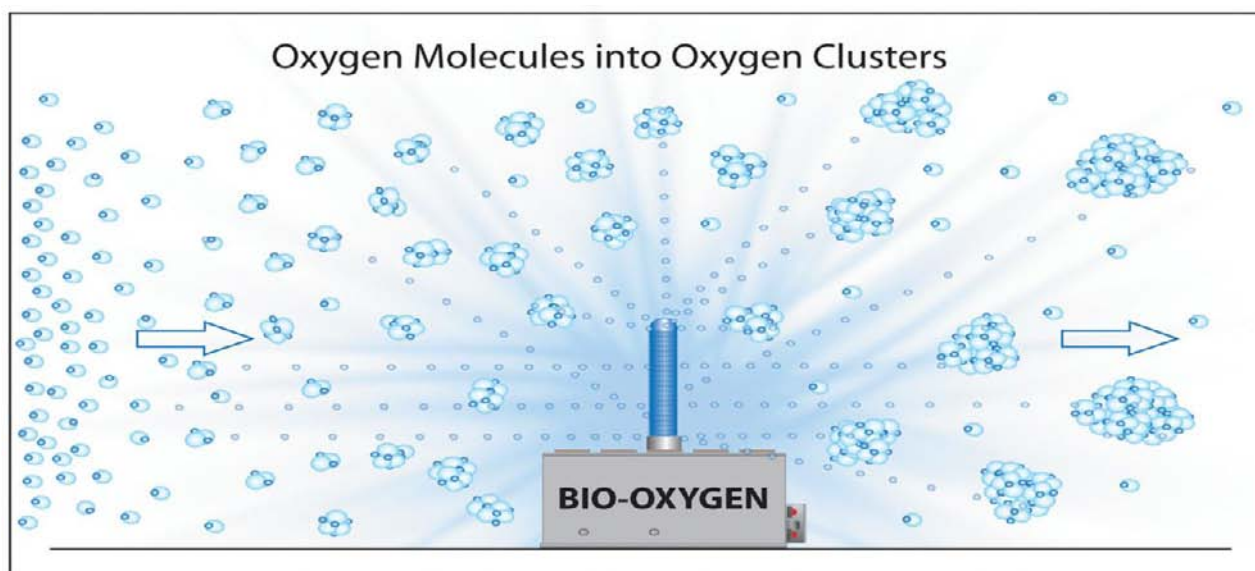
**The Bio-Oxygen Process is a process of adding extra Electrons to molecules of Oxygen.**



## THE BIO-OXYGEN PROCESS

Electricity is composed of Electrons. The Electrons are pressurised inside the 'Bio-Oxygen' Electron Tubes and are emitted in a radius of up to 2 meters around the electron tubes and produce an electron shower. As the air flows through the electron shower, the oxygen molecules absorb 1 - 4 extra electrons. When oxygen molecules gain 1 - 4 extra electrons, they become magnetic and agglomerate into Clusters composed of 2, 3, 4, 5, 6 etc oxygen molecules. Aggregates are also formed which consist of a mixture of Oxygen Clusters and ordinary O<sub>2</sub> molecules. The Oxygen Clusters and Aggregates react with and effectively remove pollutants from the air such as Odours, Gases, Chemicals, Tobacco Smoke, Nicotine and Tar and kill Bacteria, Fungus, Yeast, Mould, Mildew, Spores, Viruses, Protozoa and other Organisms. As the oxygen molecules gain extra electrons, they lose energy and drop in temperature and therefore Oxygen Clusters are colder than the Nitrogen in the air. The temperature differential between the oxygen and nitrogen in the air imparts a tinge of freshness into the room air.

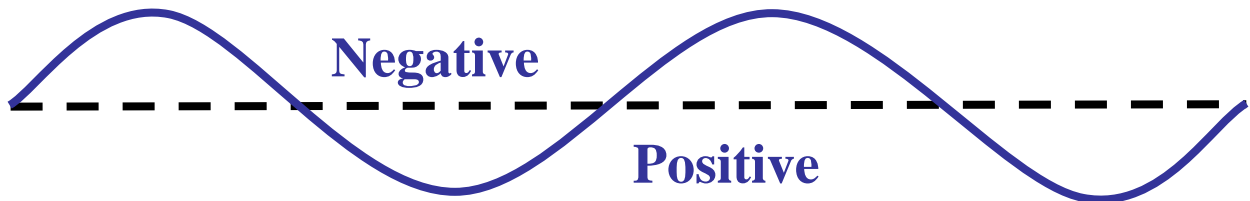
How magnetic and reactive an oxygen molecule becomes depends on the number of extra electrons that the oxygen molecule has captured. An oxygen molecule with 1 extra electron will be magnetically attracted to another with 2 extra electrons and one with 2 extra electrons will be magnetically attracted to one with 3 extra electrons and so on. At the core of each Oxygen Cluster is an oxygen molecule with the highest number of electrons. Bio-Oxygen units are fitted with a Rotary Selection Switch which enables the size of the Oxygen Clusters to be varied from small to large clusters in 11 steps because different chemicals, odours and micro-organisms require different size Oxygen Clusters to be removed. Refer to "Some common Air Pollutants oxidisable by the Bio-Oxygen Process".



## THE 'BIO-OXYGEN' PROCESS IS A NATURAL PROCESS

The Bio-Oxygen Process is the most natural of processes because the same process occurs in nature. In nature, the sun emits electrons and showers the earth with electrons. The electrons from the sun can only be absorbed by the oxygen in the atmosphere because oxygen is the only gas that is 'paramagnetic' and is able to absorb the electrons from the sun. As the oxygen molecules gain extra electrons, they become magnetic and agglomerate into Oxygen Clusters consisting of 2, 3, 4, 5, 6 etc. oxygen molecules. The Oxygen Clusters, in turn, clean the world's atmosphere of all the pollution produced in the world. **Therefore, a Bio-Oxygen unit acts like a miniature Sun in the ducts.** The Bio-Oxygen Process requires no Perfumes, Disinfectants, Chemicals or Catalysts and none are used. Bio-Oxygen does not incorporate a Carbon Filter. We require only clean ambient air.

## 'NEGATIVE' ELECTRONS COUNTERACT 'POSITIVE' STATIC ELECTRICITY



The Positron in an Atom has a positive charge and the Electrons that spin around the Positron have a negative charge and therefore Electrons, by nature, are negatively charged. The Bio-Oxygen equipment runs on AC electricity and therefore ordinarily, the discharge from the Electrode Tubes would be expected to produce 50% Positive and 50% Negative Ions. In other words, the 50% Negative Ions would be cancelled out by the 50% Positive Ions so that the overall discharge would be zero. However, a University Static Electricity Test revealed that the Bio-Oxygen Electrode Tubes discharge only Negative Electrons. This University test confirms the whole Bio-Oxygen Process because it shows that the Electron Tubes emit Electrons and that the Electrons are 'Negative'.

## ODOURS, GASES, CHEMICAL FUMES & VAPOURS



The Bio-Oxygen Process removes Odours, Gases & Chemicals in 5 -15 seconds.

### Organic Odours from:

Sewage, Urine, Faeces, Vomit, Body Odour, Toilets, Garbage, Fertilizers, Cooking, Fermentation, Spoilage and Rotting etc.

### Chemical Odours from:

Chemicals, VOC, Paints, Varnishes, Thinners, Adhesives, Glues, Plastics, Waxes, Carpets, Disinfectants, Deodorants and Perfumes etc. and from thousands of other chemicals, substances and material used and stored in buildings and factories.

## BACTERIA, FUNGUS, YEAST, MOULD, MILDEW, SPORES, VIRUSES & PROTOZOA

Oxygen Clusters are charged with extra electrons and when an organism is engulfed by Clusters of Oxygen then the body of the organism constitutes the Earth Point or lower potential against which all the surrounding Oxygen Clusters discharge their surplus electrons in a rapid short circuit discharge same as a capacitor discharges its electrons against a lower potential. The organism is continually bombarded with electrons from all sides and when the surplus electrons of one Oxygen Cluster are exhausted another cluster takes its place until the organism eventually dies from hundreds or thousands of electron shots. Organisms can develop immunity to disinfectants but there is no immunity to electron shots.

### Organisms with Soft Cell Wall

Most organisms have a soft cell wall. The organism is continually bombarded with electron shots. The electron shots easily puncture the soft cell wall and, as a result, the organism dies. Organisms with a soft cell wall are the easiest organisms to kill. The MRSA organism, Staphylococcus Aureus, has a soft cell wall and is one of the easiest organisms to kill with the Bio-Oxygen Process.

Organisms with Tough Cell Wall

Spores have a tough cell wall. In order to kill spores, they would have to be boiled in a pressure cooker for 2 hours at 120 C. Boiling at 100C for hours will not kill spores. Spores are continually bombarded with electron shots until the cell wall is punctured or cracked and, as a result, the spore dies.

Organisms with Hard Cell Wall

Some organisms have a Hard Cell Wall. The organism is continually bombarded with electron shots until the cell wall is punctured or cracked and, as a result, the organism dies.

Organisms with Lipid Envelope

Some organisms have a lipid envelope. Lipids are fats and are very easily oxidised and once the lipid envelope is oxidised, the organism is exposed and dies.



Bacteria

Anaerobic Bacteria

Anaerobic Bacteria live in an environment devoid of oxygen and to anaerobic bacteria even ordinary oxygen is toxic. When anaerobic bacteria is engulfed in clusters of oxygen composed of 100% pure oxygen and is bombarded with electrons shots, it quickly dies.

Aerobic Bacteria

Aerobic Bacteria live in normal air containing 21% oxygen, however, when aerobic bacteria is engulfed in clusters of oxygen composed of 100% pure oxygen and is continually bombarded with electron shots, it quickly dies.

How long does it take to kill a Micro-organism

(A) The speed with which an organism is killed depends mainly on the size of the organism. The larger the organism, obviously the more electron shots it can take and the smaller the organism, the less electron shots it can take. For instance, Protozoa are the largest micro organisms and therefore can take the most electron shots, whilst Viruses are the smallest organisms and can only take a few electron shots. Viruses are 100 - 1000 times smaller than Bacteria. On a time scale, Bacteria are killed in a few minutes whilst Viruses are killed in a few seconds.

(B) The length of time also depends on whether the organism has a soft, tough or hard cell wall because it takes time for the electron shots to puncture or crack a tough or hard cell wall. Don't forget that it takes minimum 2 hours of boiling in a pressure cooker at 120 C to kill spores and it takes just as long for the Bio-Oxygen Process to kill spores at ambient temperature.

**MICROBIOLOGICAL INDUCED CORROSION (MIC)**

There are micro-organisms that eat Metals, Plastics, Timber, Cement and most other materials. MIC causes wood rot. Many plastics are bio-degradable. MIC causes concrete to crumble. Many Concrete and Steel Structures have to be replaced prematurely because MIC was not recognized.

Which organisms cause MIC

Various organisms cause microbiological induced corrosion, such as:

- Sulphate Reducing Bacteria (SRB) found in sewerage systems,
- Acid Producing Bacteria (APB) found in sewerage systems.
- Iron Oxidising Bacteria (IOB) found in sewerage systems and air conditioning ducts.

**The Bio-Oxygen Process kills the organisms that cause Microbiologically Induced Corrosion.**

**COCKROACHES & RODENTS**

Cockroaches and Rodents live in a foul and smelly environment and absolutely hate the super fresh smell of Oxygen Clusters and therefore after a short time they usually leave a Bio-Oxygen treated area and migrate to another area. The Bio-Oxygen Process effectively repels Cockroaches and Rodents from kitchens, food storage and food processing areas.



## **FREE RADICALS & OH RADICALS**

Free Radicals and OH Radicals are atoms and molecules that are deficient in electrons and therefore they steal electrons from other stable molecules. When a stable molecule loses electrons, it becomes a Free Radical itself and begins a chain reaction. The Bio-Oxygen Process produces clouds of electrons and as the Free Radicals and OH Radicals flow through the electron shower, they receive all the electrons they need and therefore the Bio-Oxygen Process extinguishes Free Radicals. Free Radicals and OH Radicals cannot exist in a Bio-Oxygen installation. Free Radicals are detrimental to good health and have been associated with Cancer, Heart Disease and Premature Aging.

## **CARBON DIOXIDE**

Carbon Dioxide (CO<sub>2</sub>) decays naturally at a certain rate, however, the Bio-Oxygen Process speeds up the decay of Carbon Dioxide and therefore Carbon Dioxide levels are lower in a Bio-Oxygen treated area than in a non-treated area. Bio-Oxygen is an environmentally green process because it enhances the decay of carbon dioxide.

## **PARTICULATES & CIGARETTE ASH PARTICLES**

The Bio-Oxygen Process does not remove Dust, Particulates and Cigarette Ash Particles but that is the function of the Air Conditioning Filters anyway. In conjunction with Bio-Oxygen, we specify the following Return Air Filters:

### Smoking Rooms

Cigarette Ash Particles are up to 0.10 micron in size and therefore if the return air filter is coarser than 0.10 micron then the cigarette ash particles will pass straight through such a coarse filter and will build-up in the room and will become visible as dust haze. Therefore, for the removal of airborne Cigarette Ash Particles, we specify Air Filters that are certified to remove minimum 40% of 0.10 micron particles in one pass. Standard F5 Grade Air Filters only remove particles down to 0.30 micron and therefore 0.10 micron Cigarette Ash Particles will pass straight through such a coarse filter and will build-up and will form a dust haze in the room. If a customer installs wrong F5 grade filters in a smoking room then the customer shall be responsible for the dust haze thereby produced. Special 0.10 micron Cigarette Ash Filters are available from Bio-Oxygen.



### Non-Smoking Rooms

For Non-Smoking rooms, for the removal of ordinary Particulates and Dust, we specify 0.10 micron filters that are certified to remove minimum 20% of 0.10 micron particles in one pass. This filter is very good for desert areas because it removes fine dust particles which cause breathing difficulties. Standard F5 filters are too coarse because they only remove particles down to 0.30 micron and the dust then settles inside the building.

## **SICK BUILDING SYNDROME**

Healthy air has an excess of Negative over Positive Ions. As the air in a building is re-circulated and is pumped through the ducting system, the friction of the air against the ducts destroys the Negative Ions which results in an excess of Positive Ions. Negative Ions are healthy whilst Positive Ions are detrimental to good health. As the Positive Ions increase, people in hermetically sealed buildings begin to get tired, become more irritable and lose concentration. The Bio-Oxygen Process is the antidote to Positive Ions and Sick Building Syndrome because it injects clouds of Negative Electrons into the supply air which counteract the Positive Ions and freshen and invigorate the room air and take away tiredness and loss of concentration of workers working long hours. Tired people can't concentrate and therefore are more likely to make mistakes. Mistakes cost time and money to correct and reflects badly on your company's image.



*Hermetically sealed buildings in City of Sydney (viewed from Darling Harbour)*

## **BREATHING DIFFICULTIES**

Many people have a constantly blocked nose or constant sniffles or have a constant cough and have difficulty breathing, especially when breathing air-conditioned air. The super fresh Oxygen Clusters clear the breathing passages and enable better breathing. Affected workers like coming to work because they can breathe better at work than anywhere else.



*Tired Worker*

## **'HEPA' FILTER v BIO-OXYGEN**

HEPA Filters are "High Efficiency Particulate Arresters". They remove Dust, Particles and Micro-Organisms larger than 0.30 micron. However, particles and organisms smaller than 0.30 micron pass straight through the HEPA filter even if the efficiency of the HEPA filter is 99.99%. Together with the Bacteria, the HEPA Filters also remove particulates which consist mainly of organic material. As the organic material builds up in the pores of the HEPA Filters, it provides a source of food for the trapped organisms. In a short time, the HEPA Filters become a breeding ground and become overgrown with all sorts of micro-organisms and the HEPA Filters themselves become a source of infection. As the air flows through the infected HEPA Filters, Bacteria, Fungus, Yeast, Mould, Mildew, Spores and Protozoa are continually dislodged from the downstream side of the HEPA Filters and are blown into the room. Viruses cannot be removed even with a 99.99% efficiency HEPA Filters because they are 100 – 1000 times smaller than the 0.30 micron pore size of the HEPA Filter and therefore they pass straight through a HEPA Filter.

## **RESPIRABLE PARTICLES & CLEAN ROOMS**

Respirable Particles are microscopic particles in the size range from 0 to 0.10 micron and consist mainly of organic material. In Clean Rooms, standard 0.30 micron HEPA Filters are generally used to remove Respirable Particles but the HEPA Filters can only remove particles down to 0.30 micron and for this reason, HEPA Filters are virtually useless in Clean Rooms because you cannot remove 0 - 0.10 micron particles with a 0.30 micron HEPA Filter.

### Standard HEPA Filters (0.30 micron)

Standard HEPA Filters remove particles down to 0.30 micron and therefore smaller particles pass straight through a HEPA Filter and accumulate in the room and eventually the particles fall out and contaminate the products being produced or processed in the clean room, such as Computer Chips, Micro Tracks on Circuit Boards and Medicines. The fall-out of airborne particles can cause up to 80% of products to be rejected.

### Dust produced in Clean Room

The airborne Dust in a Clean Room is actually produced in the Clean Room itself by the processes and the activity and the people inside the Clean Room. The dust that is produced in the clean room cannot be removed by the HEPA Filters in the fresh air intake because the HEPA Filters only filter the Fresh Air going into the room and do not and cannot remove the dust being produced in the room itself because the air in the Clean Room is not re-circulated over the HEPA Filters. The air conditioning of a clean room is a flow-through system and not a re-circulating system.

### Special 0.10 micron Bio-Oxygen HEPA Filters

When we install Bio-Oxygen equipment in a clean room, we also recommend that our special 0.10 micron Bio-Oxygen HEPA Filters are installed in conjunction with our equipment. Respirable Particles smaller than 0.10 micron particles consist mainly of organic material which are oxidisable and are effectively removed by the Bio-Oxygen Process. Our special HEPA Filters remove particles larger than 0.10 micron and the Bio-Oxygen Process removes particles smaller than 0.10 micron. If we reduce the fall-out of particles in your Clean Room by up to 90% then we will also lower the product rejection rate by up to 90%.

### Extend Service Life of HEPA Filters

If the Bio-Oxygen units are installed upstream from the HEPA Filter then the Oxygen Clusters will oxidise most of the trapped organic material in the pores of your HEPA Filters and will maintain the airflow through the HEPA filter longer. As a bonus, Bio-Oxygen is likely to double the life of your HEPA Filters. This will cut your HEPA Filter replacement cost by up to half. Furthermore, the Oxygen Clusters not only remove Respirable Particles but also remove Odours, Gases and Chemicals which the HEPA Filter cannot remove.

In addition to that, the Oxygen Clusters also kill Bacteria, Fungus, Yeast, Mould, Mildew, Spores, Viruses, Protozoa and other Micro-Organisms in the air and on surfaces in the Clean Room which is also beyond the ability of any HEPA Filter.

### Bio-Oxygen

By comparison, the Bio-Oxygen Process re-arranges the oxygen molecules in the Clean Room into Oxygen Clusters and the Oxygen Clusters, in turn, oxidise the airborne Respirable Particles smaller than 0.10 micron in the room air whilst the Bio-Oxygen HEPA filters remove particles larger than 0.10 micron. The Oxygen Clusters oxidise the Respirable Particles as the particles are produced and float in the room air.

The Oxygen Clusters remove Respirable Particles in mid air in up to 1 minute (depending on size) and therefore the concentration of Respirable Particles in a Clean Room can only be as much as can be produced in the room in up to 1 minute. For the Oxygen Clusters, the smaller the particle, the easier and the faster it is oxidised and therefore a 0.001 micron particle is easier and faster removed than a 0.10 micron particle. For filters, the opposite applies, the smaller the particle, the more difficult it becomes to remove with a filter. In any event, there is no filter anywhere in the world that is able to remove particles smaller than 0.10 micron and 0.10 micron is definitely the limit, even for HEPA Filters. However, for the Bio-Oxygen Process, 0.10 micron is only the starting point. The Bio-Oxygen Process oxidises particles from 0 – 0.10 micron in less than 1 minute.

### 100% Outside Air

Usually, in order to prevent the build-up of Particulates or Bacteria in a Clean Room, the air conditioning system is always a flow-through system that uses 100% outside air. The theory is that the more air flows through a Clean Room, the faster particulates and bacteria will be flushed out of the room. The air conditioning system usually provides minimum 20 air changes per hour or 1 air change every 3 minutes. The conditioned air comes in on one side of the room and after 3 minutes is exhausted at the other side of the room. Therefore, air conditioning system of a clean room is a 100% wasteful system because it wastes 100% of the conditioned air. An air conditioning system that uses 100% outside air will run flat out 100% of the time and therefore the compressors consume an excessive amount of power and wear out faster and as a result, also break down more often. The harder that the air conditioning has to work and the more electricity it consumes, the faster the equipment wears out and the more often the equipment breaks down, resulting in unnecessary down-time and extra maintenance and repair costs and faster equipment depreciation.

### 80% Return Air

By comparison, with Bio-Oxygen, you can run the air conditioning system of your Clean Room as a normal return air system, with up to 80% Return Air and as little as 20% Outside Air. As you reduce the outside air intake from 100% Outside Air to 20% Outside Air, your air conditioning compressor will run on idle and the power consumption will accordingly drop by up to 50%. The savings in electricity and reduced wear and tear of your air conditioning compressors and reduced break-downs will pay for the Bio-Oxygen equipment. Our special HEPA Filters will remove particles larger than 0.10 micron and Bio-Oxygen will remove particles and organisms smaller than 0.10 micron (from 0 to 0.10 micron). We can give you much cleaner air with 80% return air than you are currently getting with 100% outside air. Your Clean Room is dirty in relation to what Bio-Oxygen can give you.

## **CARBON FILTER versus BIO-OXYGEN**

Carbon Block Filters or Carbon Granule Filters are often used to remove Odours, Gases and Chemicals. Carbon Blocks are shaped like a house brick and have pores like wormholes. The wormholes go from side to side through the carbon block. The carbon blocks are stacked one on top of another like a brick wall. A powerful fan blows the polluted air through the carbon filter.

### Carbon must be kept dry

The carbon must be kept dry because once the pores of the carbon are full of water, they cannot hold water and gases as well. The pores can either hold water or gas but they cannot hold both. For this reason, a Dehumidifier is required for a Carbon Filter installation to keep the carbon dry. The dehumidifier must have the same capacity as the ventilation fan. Without a dehumidifier, a carbon filter would be useless.

### Contact Time

As the Odours, Gases and Chemicals flow through the carbon bed, they make contact with the carbon and are absorbed into the pores of the carbon, so the theory goes. The minimum required contact time for the odours and gases to be absorbed into the carbon is 0.20 seconds, provided that the carbon is dry. If the pores of the carbon are already full of water then, of course, the carbon can't hold odours and gases as well. However, the problem is that as the polluted air is blown through the carbon granule bed, the air follows the path of least resistance and therefore the polluted air tends to flow along the gaps around the granules rather than through the pores of the carbon granules. For this reason, carbon granule filters only have a relatively low efficiency.

### Exhaust Temperature

Gases expand and contract depending on temperature. Therefore, the capacity of carbon to hold gases in the pores of the carbon depends on the temperature of the exhaust gases and the environmental temperature. As the temperature goes up, the trapped gases in the pores of the carbon expand and begin to get squeezed out of the pores. Some of the odours and gases that are absorbed during the night are squeezed out again during the day. The higher the temperature of the exhaust gases, the lower the absorption capacity of the carbon filter will be. With carbon filters, the temperature of the exhaust gases should be kept (a) constant and (b) as low as possible, ideally below 30 C, however, in reality this is not possible.

### Airborne Particulates block Pinholes

The pores of carbon block or carbon granule filter are very easily blocked by airborne particulates and once a pore is blocked, it cannot absorb any more odours and gases. Gradually, as more and more of the pores are blocked, the odour absorption capacity of the carbon is accordingly impaired and it is only a question of time before most the pores are blocked and the odour absorption capacity of the carbon comes virtually to an end. Mostly the pores are blocked before the carbon has reached its maximum absorption capacity.

### Bio-Oxygen

By comparison, the Bio-Oxygen Process injects Oxygen Clusters into the exhaust stack. The Oxygen Clusters react with the Odours, Gases and Chemicals in the exhaust duct in 5 – 15 seconds. The electron tubes are always installed in the path of clean outside air and the polluted air does not flow over the electron tubes and therefore the electron tubes always stay clean. Once the Oxygen Clusters have bonded with an odour molecule, the Oxygen Clusters continue to act on the odours, gases and chemicals in mid air and the odours gradually diminish over 5 – 15 seconds. The odours can only travel as far as the air currents and wind can carry the odours in 5 – 15 seconds but along the way, the odours gradually diminish and become weaker and weaker until in 15 seconds, the odours are gone. The Bio-Oxygen Process is a positive process because it actually causes a chemical reaction between the Oxygen Clusters and the odours, gases and chemicals. The Bio-Oxygen Process is a positive process that works at the molecular level. Carbon Filters are a negative system because they only absorb odours and don't do anything to the odours and chemicals themselves. An equivalent Carbon Filter would cost about twice as much as a Bio-Oxygen system. The maintenance costs of a Carbon Filter are also about twice as much as for Bio-Oxygen and the performance and efficiency of a Carbon Filter is lower and on a declining curve whereas the Bio-Oxygen Process remains constant for the duration of the service period.

## **BIO-OXYGEN** *-The Natural Process*

Mr John B. Waanders  
Laboratory Manager, Department of Chemical Engineering  
The University of Newcastle, Callaghan, NSW 2308  
Phone: (02) 4921 6103 Fax: (02) 4921 8692  
13<sup>th</sup> July 2006

Mr Philipp Leicher  
Bio-Oxygen Australia Pty Limited  
36 Bennett Place  
Castle Hill 2154

Re: Oxygen Clusters

Dear Philipp,

You mentioned that from time to time people ask whether Oxygen Clusters are safe.

Oxygen is present in the atmosphere at a concentration of ~21% (210,000 ppm oxygen). Oxygen Clusters that are formed by the Bio-Oxygen Process do not alter the overall concentration of the oxygen in the air and the oxygen will still only remain in the air at a concentration of up to 21%. The Bio-Oxygen Process merely re-arranges the oxygen molecules into Oxygen Clusters but does not change the overall concentration of the oxygen in the air. Oxygen Clusters are formed when the oxygen molecules gain electrons.

The presence of oxygen in the form of Oxygen Clusters does not in any way create a condition that can be considered hazardous to human and animal health, and in my professional opinion I am sure that Oxygen Clusters are actually quite beneficial to good health.

Yours faithfully

A handwritten signature in black ink that reads "John Waanders". The signature is written in a cursive, flowing style.

John Waanders, BE, MEngSc, FIEAust, CPEng, FICChemE, CEng.



**BIO-OXYGEN**  
**AUSTRALIA PTY. LIMITED**

36 Bennett Place, Castle Hill NSW 2154, Australia

Phone: (61) 2 9899 7059 ABN: 73 003 380 185 Fax: (61) 2 98993161

Email: bio-oxy@bigpond.net.au Web: www.bio-oxygen.com.au



Scientific References:

## **MAGNETIC PROPERTIES OF OXYGEN**

[6] "Encyclopaedia Britannica" 1965, Volume 16, p 1192

***"Oxygen is paramagnetic in all its physical states".***

[4] W.R. Keen, M.J. Rogers and P. Simpson, "Chemistry, Facts, Patterns & Principles" Addison-Wesley (1972). p 436.

***"Oxygen has a bond order of two (from the bond length and bond enthalpy) and shows paramagnetism equivalent to two unpaired electrons".***

[5] D.P. Shoemaker, C.W. Garland and J.I. Steinfeld, "Experiments in Physical Chemistry" (3<sup>rd</sup> Edition), McGraw Hill (1974), p 424.

***"In molecular Oxygen O<sub>2</sub>, two molecular orbitals of equal energy each contain a single electron in accordance with Hund's first rule; consequently, oxygen gas is paramagnetic".***

[1] "Funk & Wagnalls Encyclopedia" (1969), Volume 18, p 6808.

***"Ordinary oxygen is a colorless, odorless, tasteless, slightly magnetic, non-toxic gas, with specific gravity 1.105. It can be condensed to a pale-blue liquid, b.p. – 183<sup>o</sup>C (-297<sup>o</sup>F), which is strongly magnetic".***

[2] "Microsoft Encarta 96, Encyclopedia", CD-ROM, 1996 Edition, Microsoft Corporation.

***"Oxygen, symbol O, colorless, odorless, tasteless, slightly magnetic gaseous element." & Gaseous oxygen can be condensed to a pale blue liquid that is strongly magnetic."***

[3] R.C. West and M.J. Astle, "Handbook of Chemistry and Physics" (63<sup>rd</sup> Edition), CRC Press (1982), p B-29.

***"the gas is colorless, odorless and tasteless. The liquid and solid forms are a pale blue color and are strongly magnetic".***

[7] Dept. of Chemistry, Hoyt Laboratory, Princeton University and Institute of Basic Biological Problems, Russian Academy of Sciences, 2000, G.C. Dismukes, V.V. Klimov, S.V. Baranov, Yu. N. Kozlov, J. DasGupta and A. Tyryshkin, ***"The origin of Atmospheric Oxygen on Earth: The innovation of oxygenic photosynthesis."***



Scientific References:

## **OXYGEN CLUSTERS**

[1] Uppsala University, Department of Physics, Physics 5: Surface Physics ***“Clusters are aggregates of a small and finite number of atoms or molecules. They range from the dimer, consisting of only 2 atoms, up to large clusters made up of several tens of thousands of atoms”***

[2] Journal of Low Temperature Physicsw 2001, Vol. 122, Issue 3-4, 179 – 186, Y. A. Freiman, A. Jezowski, A.P. Brodyanski, V.V. Sumarokov, Z. Litwicki, ***“Magnetic Properties of Oxygen Clusters”***.

[3] University of California, San Diego, Faraday Discussions, 1997, 108, 115 – 130, Runjun Li, Karl A. Hanold, Mark C. Garner, A. Khai Luong and Rober E. Continetti ***“Excited state dynamics in Clusters of Oxygen”***.

[4] Institut fur Ionenphysik, Leopold Franzens Universitat, Innsbruck, Austria, Physical Review Letters, Volume 77, Number 18, 1996, ***“Vibrationally resolved electron attachment to Oxygen Clusters”***.

[5] Institut fur Ionenphysik, Leopold Franzens Universitat, Innsbruck, Austria, Journal of Chemical Physics, Volume 111, Number 8, 1999, 3548 – 3558, S. Metejcik, P. Stampfli, A. Stamatovic, P. Scheier and T.D. Mark, ***“Electron Attachment to Oxygen Clusters studied with high energy resolution”***.

[6] Journal Chem. Soc., Faraday Transactions, 1319, 1996, Alexander Malakhovskii, Elena Sominska & Aaron Gedanken, ***“Magnetism in Oxygen Clusters, Study of pure and mixed Clusters of Oxygen”***

[7] Physical Chemistry, Chemical Physics, 4 (20) : 4970 – 4978, 2002, V. Aquilanti, E. Carmona-Novillo, F. Pirani, ***“Quantum Mechanics of molecular Oxygen Cluster: rotovibrational dimer dynamics from realistic potential energy surface.”***

[8] Institut fur Ionenphysik, Leopold Franzens Universitat, Innsbruck, Austria, Plasma Sources Sci. Technol. 6 (1997), 140 – 146, S. Metejcik, A. Kiendler, P. Cicman, J. Skalny, P. Stampfli, E. Illenberger, Y. Chu, A. Stamatovic, T.D. Mark, ***“Electron attachment to molecules and clusters of atmospheric relevance: “oxygen and ozone”***.

[9] Institut fur Ionenphysik, Leopold Franzens Universitat, Innsbruck, Austria, Arbeitsgruppe Clusters, Oberflächen, Massenspektrometrie und Lebensmittelanalyse, Journal Chem. Phys. 116 (2002), 7583 – 7588, S. Matt, R. Parajuli, A. Stamatovic, P. Scheier, T.D. Mark, ***“Quantitative investigation of the kinetic energy release in metastable decay reaction of (O<sub>2</sub>)<sup>+</sup> ions: Evidence for a change in the metastable decay mechanisms as a function of cluster size”***.

## Magnetic Properties of Oxygen Clusters

Yu. A. Freiman<sup>1</sup>, A. Jeżowski<sup>2</sup>, A. P. Brodyanski<sup>3</sup>,  
V. V. Sumarokov<sup>1</sup>, and Z. Litwicki<sup>2</sup>

<sup>1</sup>*B. Verkin Institute for Low Temperature Physics and Engineering,  
Natl Acad. Sci. of Ukraine, 47 Lenin Ave., Kharkov, 310164, Ukraine*

<sup>2</sup>*W. Trzebiatowski Institute of Low Temperature and Structure Research,  
Polish Acad. Sci., 50-950 Wrocław 2, P.O.Box 1410, Poland*

<sup>3</sup>*University of Kaiserslautern, Physics Department,  
Erwin-Schrödinger-Str., D-67653, Kaiserslautern, Germany*

*Magnetic properties of oxygen pair clusters are investigated theoretically for different geometries of clusters which can be realized by doping molecular cryomatrices with oxygen. Anomalous temperature and pressure behavior of the magnetic susceptibility, magnetic heat capacity and magnetic entropy is predicted. It is shown that the low-temperature magnetic susceptibility of these solid solutions is very sensitive to the orientational structure of impurity oxygen clusters, which makes it possible to use the susceptibility data for studying structural and dynamics properties of the host lattice, including high-pressure phases of simple molecular crystals.*

The study of properties of cryocrystals doped with impurities is a well-known source of information about the impurity molecules isolated in the matrix. At the same time, a rich information can be extracted from these studies on matrix lattice dynamics, and about the interaction of impurity molecules with the matrix and with each other.

One of the most interesting in this aspect is oxygen molecules which are frequently employed as a probe of properties of atomic and molecular cryocrystals. A number of studies was devoted to anomalies in specific heat, thermal expansion and thermal conductivity due to oxygen impurities [1-7]. This note is devoted to unusual magnetic properties of oxygen clusters.

Compared with ordinary magnets, magnetic systems containing magnetically active molecules or molecular groups can exhibit unusual magnetic

properties [8,9]. The magnetic Hamiltonian in this case contains a new variable, the angle between molecular axis. Solid oxygen and some alkali-hyperoxides are examples of such magnetic systems.

The spin Hamiltonian of exchange-coupled clusters of oxygen molecules can be written in the form [2-5]:

$$\mathcal{H} = \sum_i \left[ D(S_i \vec{n}_i)^2 - \frac{1}{3} \vec{S}(\vec{S} + 1) \right] + \frac{1}{2} \sum_{ik} J_{ik} S_i S_k, \quad (1)$$

where  $D$  is the spin-figure constant,  $\vec{n}_i$  is the unit vector directed along the molecular axis,  $\vec{S}$  is the spin operator ( $S = 1$ ),  $J$  is the exchange parameter.

For free oxygen molecules  $D = 5.718$  K [10]; for matrix-embedded molecules the constant  $D$  can be renormalized [1-5,11]. The parameter  $J/D$  for the  $N_2$ - $O_2$  solid solution at zero pressure is a value of order of unity, but for different matrices - and as a function of pressure - it can vary in wide limits. The third characteristic parameter of the Hamiltonian (1), the angle between the axis of oxygen molecules, is matrix-dependent. For the case of the fluorine matrix, the angle  $\theta$  is close to zero (the collinear cluster), for the case of the  $\alpha$ -nitrogen matrix,  $\theta \approx \arccos(1/3)$ , for the case of  $\gamma$ -nitrogen,  $\theta \approx \pi/2$  (the orthogonal cluster).

For the Hamiltonian (1) we obtained exact analytical expressions for the contribution of pair impurity clusters to magnetic susceptibility, magnetic heat capacity and magnetic entropy. Exact analytical expressions for these magnetic characteristics can be expressed in terms of the eigenvalues  $E_i$  of the Hamiltonian (1) and coefficients  $a_{i_1}$  and  $a_{i_2}$  which determine first- and second-order energy corrections in the perturbation theory with the Zeeman energy as a perturbation term. In particular, the zero-field magnetic susceptibility

$$\chi T = \frac{(\mu_B g)^2}{Z} \left[ \frac{1}{T} \sum_i a_{i_1}^2 e^{-E_i/T} - 2 \sum_i a_{i_2} e^{-E_i/T} \right], \quad (2)$$

where  $\mu_B$  is the Bohr magneton,  $g$  is the splitting factor ( $g = 2$ ),  $Z = \sum_i e^{-E_i/T}$  is the statistical sum of the system.

We will consider here a number of particular cases.

### Collinear cluster ( $\vec{n}_1 \parallel \vec{n}_2$ )

Zero-temperature transverse susceptibility

$$\chi_{xx} = \chi_{yy} \equiv \chi_{tr} = \frac{4}{D} (\mu_B g)^2 \frac{(1 + E_0/2J)^2}{1 + 2(E_0/2J)^2} \frac{D/J}{(1 + D/J - E_0/J)}, \quad (3)$$

where  $E_0$  is the ground-state energy

$$\frac{E_0}{J} = -\frac{1}{2} + \frac{D}{J} - \sqrt{\frac{9}{4} - \frac{D}{J} + \left(\frac{D}{J}\right)^2}.$$

Low-temperature behavior of the parallel susceptibility is given by equation

$$\chi_{zz}(T \rightarrow 0) = 2(\mu_B g)^2 \frac{1}{T} \exp \left[ -\frac{1}{T}(D - J - E_0) \right]. \quad (4)$$

Zero-temperature powder susceptibility  $\{\chi_p = \frac{1}{3}(\chi_{xx} + \chi_{yy} + \chi_{zz})\}$  in the limits of small and large exchange parameter are given by equations

$$\chi_p(T=0) = \frac{8}{3}(\mu_B g)^2 \frac{1}{D} \begin{cases} 2(1 - 2J/D), & J/D \ll 1 \\ \frac{4}{81}(J/D)^{-3}, & J/D \gg 1 \end{cases}. \quad (5)$$

#### Orthogonal cluster ( $\vec{n}_1 \perp \vec{n}_2$ )

This is the most peculiar case, since at  $J/D = 3/4$  there is a crossing of the two lowest magnetic levels which results in anomalous behavior of all the magnetic properties (see Figs. 1-4).

Zero-temperature behavior of the three components of the magnetic susceptibility in the limits of small and large exchange parameter are given by the equations

$$\chi_{xx} = \chi_{yy} = \chi_{zz} = \frac{2}{D}(\mu_B g)^2 \begin{cases} 1 + \frac{3}{8}(J/D)^2, & J/D \ll 1 \\ \frac{2}{81}(J/D)^{-3}, & J/D \gg 1 \end{cases}. \quad (6)$$

$$\chi_{xy} = \chi_{yz} = \frac{2}{D}(\mu_B g)^2 \begin{cases} 2(1 - 2J/D), & J/D \ll 1 \\ 0, & J/D > \frac{3}{4} \end{cases}. \quad (7)$$

As one can see from Fig. 1a,  $\chi_{zz}$  is a nonmonotonic function of  $J/D$ . At  $T = 0$  there is a jump at  $J/D = 3/4$ , which is smeared out with temperature. At  $T = 0$ ,  $\chi_{xx}$  exhibits a jump to the zero value at  $J/D = 3/4$  (Fig. 1b).

Behavior of the powder susceptibility is shown in Fig. 1c and for large  $J/D$  is given by equation

$$\chi_p(T=0) = \frac{8}{243D}(\mu_B g)^2 \left(\frac{J}{D}\right)^{-3}, \quad \frac{J}{D} \gg 1. \quad (8)$$

Anomalies in the behavior of spin-spin correlation functions, magnetic thermal capacity, and magnetic entropy shown in Figs. 2-4. A double-maximum Shottky-type anomaly in the magnetic thermal capacity and a peak in the magnetic entropy are a consequence of the crossing of the lowest spin levels of the system with a change of in  $J/D$ . In experiment different values

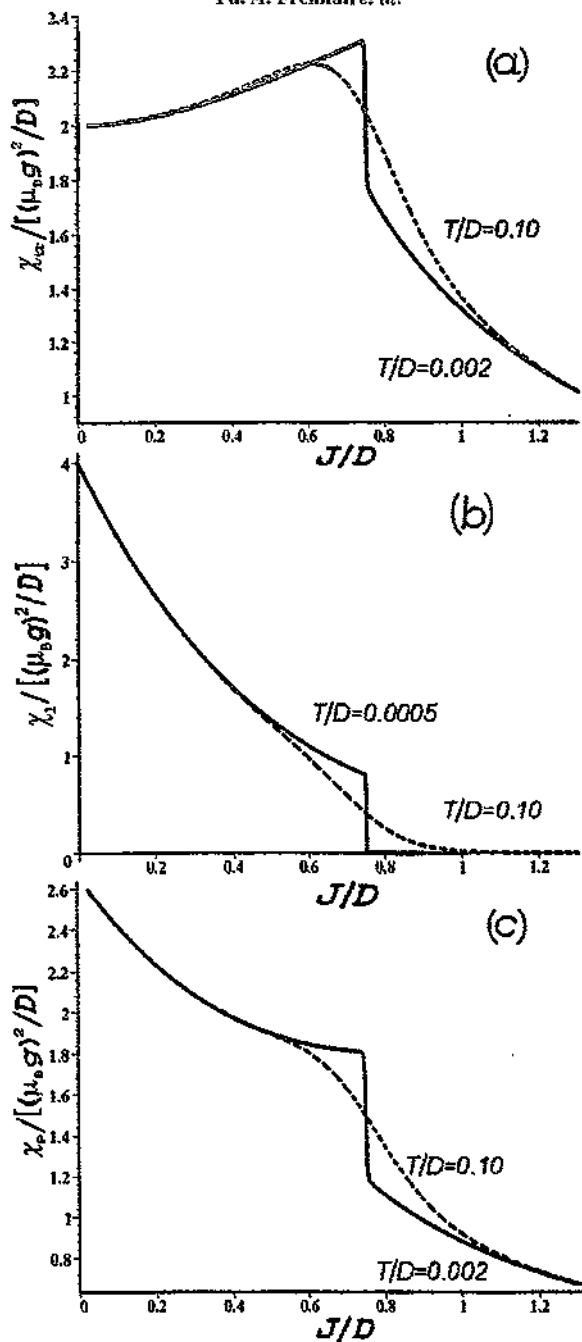


Fig. 1. Magnetic susceptibility of the orthogonal cluster: (a) - transverse, (b) - longitudinal, (c) - powder.

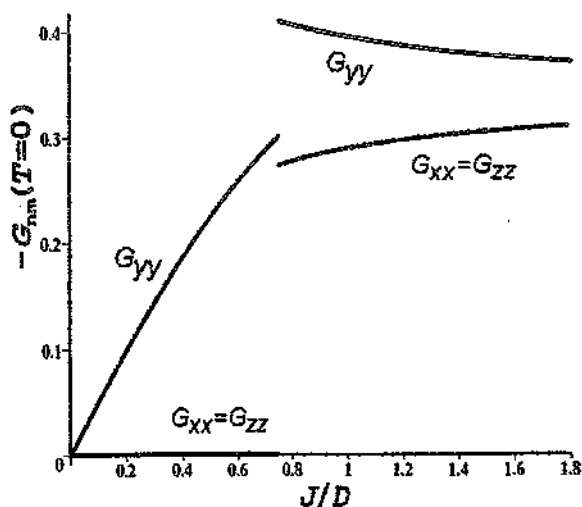


Fig. 2. Spin-spin correlation function of the orthogonal cluster.

of  $J/D$  can be obtained by changing pressure applied to the system. The same behavior of the magnetic entropy was observed experimentally in  $\text{PrNi}_3$  in Ref. [12]. Similar anomalies are characteristic not only for the orthogonal clusters but for clusters with arbitrary  $\theta$ , since there is a minimum in the  $\Delta E$  vs  $J/D$  curves, where  $\Delta$  is the gap between the two lowest spin levels. But in the absence of the crossing the anomalies are not so pronounced and Shottky anomaly in the thermal anomaly has only one peak.

Comparing (5b) and (8) we get

$$\frac{\chi_p(\vec{n}_1 \parallel \vec{n}_2)}{\chi_p(\vec{n}_1 \perp \vec{n}_2)} = 4, \quad (9)$$

which characterizes sensitivity of the magnetic susceptibility to the geometry of the impurity clusters.

The general zero-temperature angle dependence of the powder susceptibility is given by equations

$$\chi_p(\theta) = \frac{8}{3}(\mu_B g)^2 \frac{1}{D} \begin{cases} [1 - J/D(1 + \cos^2 \theta)], & J/D \ll 1 \\ \frac{1}{81}(J/D)^{-3}(1 + 3 \cos^2 \theta), & J/D \gg 1 \end{cases} \quad (10)$$

The magnetic susceptibility of a dilute solid solution could be represented as a sum of the contributions of single oxygen molecules, pairs, triples, and larger clusters

$$\chi_{\text{sol}} = N_1 \chi_1 + N_2 \chi_2 + \dots \quad (11)$$

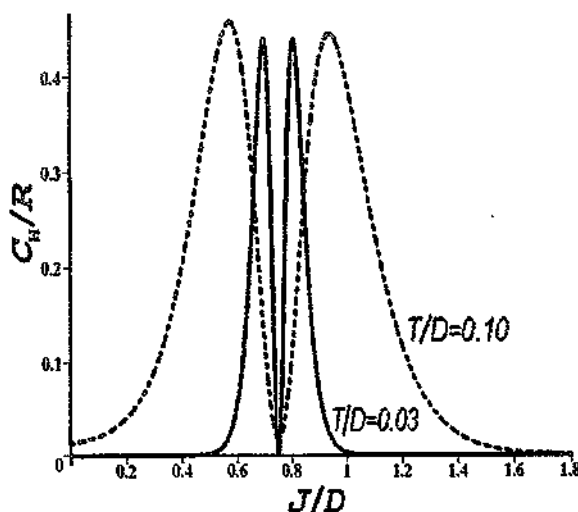


Fig. 3. Magnetic thermal capacity.

where  $N_1, N_2, \dots$  are numbers of singles, pairs, etc.,  $\chi_1, \chi_2$ , are contributions of these clusters into total magnetic susceptibility. The contribution from single oxygen molecules in the high-temperature limit is

$$\chi_1 = \frac{4}{3}(\mu_B g)^2 T^{-1} \left\{ 1 - \frac{1}{18}(D/T)^2 + \dots \right\}, \quad (12)$$

where the factor in curly brackets determines the deviation from Curie law. In the zero-temperature limit the contribution from singles is determined by a single parameter, spin-figure constant:

$$\chi_1 = \frac{4}{3}(\mu_B g)^2 D^{-1}, \quad (13)$$

which makes it possible to obtain this constant from low-temperature susceptibility data for very dilute solutions when the impurity concentration is very small and the number of pair clusters is negligible. At elevated concentrations the contribution from clusters of impurity molecules can be separated from the total susceptibility, and considering  $D$  as a known quantity, the magnitude of  $J/D$  ratio, the angle between the axis of oxygen molecules, and  $N_2$  can be found, by analyzing the deviation of the susceptibility from Curie law.

In conclusion, magnetic properties of oxygen pair clusters were investigated theoretically for different geometries of clusters. Anomalous temperature and pressure behavior of the magnetic susceptibility, thermal capacity

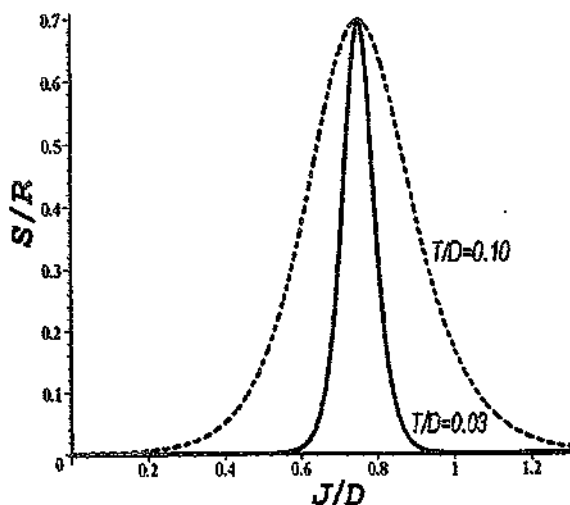


Fig. 4. Magnetic entropy of the orthogonal cluster.

and entropy is predicted. The data on these anomalies can be used for studying of distance and angular dependence of exchange interaction parameter and for analysis of the positional and orientational short order in the oxygen-doped solid solutions.

The research reported in this paper was supported by Polish Committee for Scientific Research, grant No 2 P03B 14210.

## REFERENCES

1. J.C. Burford and G.M. Graham, *J. Chem. Phys.* **49**, (1968) 763.
2. V.V. Sumarokov, Yu.A. Freiman, V.G. Manzhelii, and V.A. Popov, *Sov. J. Low Temp. Phys.* **6**, (1980) 580.
3. A. Jeżowski, Yu.A. Freiman, A.M. Tolkachev, V.P. Azarenkov, V.G. Manzhelii, and E.A. Kosobutskaya, *Sov. J. Low Temp. Phys.* **6**, (1980) 723.
4. Yu.A. Freiman, A. Jeżowski, and V.V. Sumarokov, *J. Phys. C* **19**, (1986) 5309.
5. V.S. Ostrovskii, V.V. Sumarokov, and Yu.A. Freiman, *Sov. J. Low Temp. Phys.* **12**, (1986) 116.
6. Yu.A. Freiman, V.V. Sumarokov, A. Jeżowski, P. Stachowiak, and J. Mucha, *Low Temp. Phys.* **22**, (1996) 148.
7. A. Jeżowski, P. Stachowiak, J. Mucha, Yu.A. Freiman, and V.V. Sumarokov, *High Temp. - High Press.* **29**, (1997) 423.
8. M.E. Lines and M.A. Bösch, *Comm. Solid State Phys.* **11**, (1983) 73.
9. A.P. Brodyanski and Yu.A. Freiman, *Sov. J. Low Temp. Phys.* **11**, (1985) 538.

10. M. Tinkham and M.W.P. Strandberg, *Phys. Rev.* **97**, (1955) 937.
11. Yu.A. Freiman and A. Jeżowski, *Sov. J. Low Temp. Phys.* **10**, (1984) 340.
12. P.J. von Ranke *et al.*, *Phys. Rev.* **58**, (1998) 14436.

## Vibrationally Resolved Electron Attachment to Oxygen Clusters

S. Matejcik,\* A. Kiendler, P. Stampfli, A. Stamatovic,<sup>†</sup> and T. D. Märk

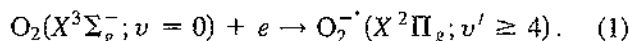
*Intitut für Ionenphysik, Leopold Franzens Universität, Technikerstrasse 25, A-6020 Innsbruck, Austria*

(Received 21 March 1996; revised manuscript received 31 May 1996)

Highly monochromatized electrons (with 30 meV FWHM) are used in a crossed beam experiment to investigate electron attachment to oxygen clusters  $(O_2)_n$  at electron energies from approximately 0 to 2 eV. At energies close to zero, the attachment cross section for the reaction  $(O_2)_n + e \rightarrow O_2^-$  rises strongly with decreasing electron energy compatible with *s*-wave electron capture to  $(O_2)_n$ . Peaks in the attachment cross section present at higher energies can be ascribed to vibrational levels of the oxygen anion. The vibrational spacings observed can be quantitatively accounted for by model calculations. [S0031-9007(96)01481-0]

PACS numbers: 36.40.-c, 34.80.Lx

Few atomic collision processes have been investigated so thoroughly as those involving the electron and oxygen molecule, including intensive studies on electron attachment [1,2]. One of the reasons for this is that reactions involving molecular oxygen and its anions are of importance in understanding atmospheric chemistry [3]. Electron attachment to a single ground state oxygen molecule proceeds in the energy range from 4.4 to 10 eV via a dissociative channel, whereas, at low energies (below 1 eV), attachment to  $O_2$  (which has a positive adiabatic electron affinity of  $EA = 0.440 \pm 0.008$  eV [4]) results in a nondissociative resonance process [5,6]



Because the bond length of the neutral molecule is much smaller than for the anion [7] and because  $O_2$  has a positive EA (see Fig. 1), the incoming electron cannot induce a Franck-Condon transition to the ground state of the anion. Instead, only vertical transitions to the fourth and higher vibrational levels of the anion are possible, the fourth vibrational level lying about 90 meV above the first vibrational level of the neutral [8]. The molecular anion formed via reaction (1) is unstable with a predicted [9] lifetime towards autodetachment of about  $10^{-10}$  s. In a high pressure environment this anion can be stabilized collisionally to a vibrational level  $v' < 4$  which lies below the  $v = 0$  level of the neutral [see Fig. 1(a)], thereby making autodetachment impossible. According to Spence and Schulz [5] and McCorkle, Christophorou and Anderson [6], the "effective" cross section for this "three-body attachment" process (proceeding via the low-lying  $^2\Pi_g$  compound state) shows pronounced structure with peak energies coinciding with the positions of the vibrational states of the  $O_2^-$  compound state with  $v' \geq 4$  (see also Ref. [10]).

Recently, electron attachment to oxygen clusters was studied in crossed beam experiments showing at low energy a broad "zero energy" peak for the production of  $O_2^-$  and higher homologues, i.e., the stoichiometric  $(O_2)_n^-$  anions [11,12] (the production of nonstoichiometric cluster anions was found to closely follow the energy

dependence of the  $O^-$  production from the monomer). The position of this zero energy resonance was reported in the earlier measurements (using electron beams with an energy distribution of 0.5 eV FWHM) to lie close to 0 eV [11], whereas, in the later experiments, using an electron monochromator with a 0.2 eV FWHM, the maximum was found to lie at about 0.7 eV [12] (it is conceivable that this difference could be due to a distinctly smaller average cluster size in the later experiment, see below).

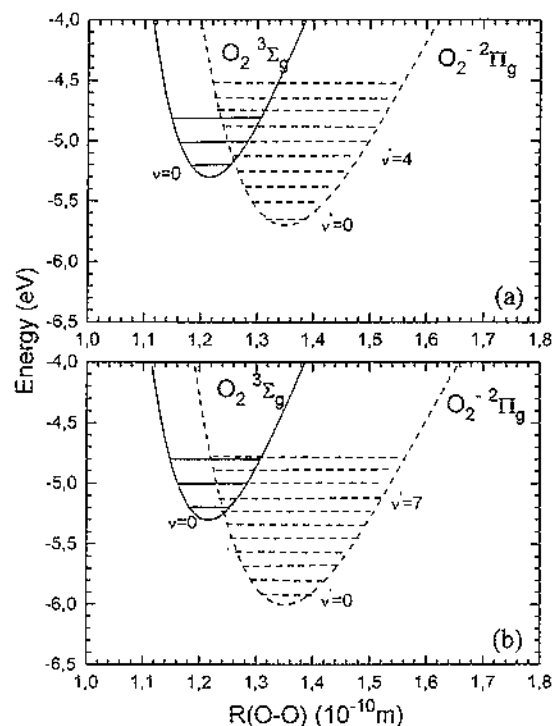


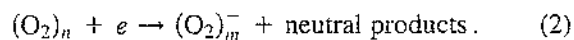
FIG. 1. (a) Approximate potential energy curves for  $O_2$  and  $O_2^-$  after Spence and Schulz [5]. The  $v' = 4$  state is located 0.091 eV above the  $v = 0$  state [8]. (b) Hypothetical potential energy curves (see text for details of the applied shift between the two curves) for  $O_2$  and  $O_2^-$  solvated in an oxygen cluster. Note that the  $v' = 7$  anion state is located in this hypothetical drawing approximately 80 meV above the  $v = 0$  neutral state in accordance with the present experimental results.

As no anions have been observed previously in electron/ $O_2$  crossed beam experiments under single collision conditions at these low energies, the question remained (besides the observed discrepancy in the peak position): What is the exact attachment mechanism leading to the production of these ions at thermal energies?—An attachment reaction of importance in low temperature and high pressure swarm experiments [2].

In this Letter we report the results of a crossed electron/oxygen cluster beam study using a recently developed high resolution electron monochromator with a possible FWHM energy spread of as low as about 5 meV [13,14]. It is thus possible for the first time to resolve vibrational structure in electron attachment cross sections of clusters. Based on a theoretical analysis of (i) the cross section dependence on electron energy and (ii) the vibrational structure, it is possible to elucidate the attachment mechanism responsible for the specific energy dependence observed, i.e., involving, at very low electron energies, nonadiabatic  $s$ -wave capture of the incoming electron and, at energies above about 80 meV, Franck-Condon governed transitions to specific vibrational levels of a single oxygen molecule within the target cluster, in both cases followed by evaporative cooling.

The molecular-beam source, electron-impact ion source, and quadrupole mass spectrometer system have been described previously [13–15]. Neutral oxygen clusters  $(O_2)_n$  are formed by the expansion of up to 5 bars of oxygen through a 20  $\mu$ m nozzle into vacuum. The stagnation gas and nozzle temperature is variable and kept constant with a closed cycle cryostat during the experiment at a typical temperature of  $-140^\circ\text{C}$ . The highly monochromatized electron beam is produced in a trochoidal monochromator especially designed [13,14] to achieve high resolution (in the present case using 30 meV FWHM, thus giving electron currents of 30 nA which are large enough to allow the study of electron capture reactions close to 0 eV). The anions produced in the collision region are extracted on line to the direction of the neutral cluster beam by a weak extraction field thus minimizing artifacts in the measured attachment cross section functions [16]. The zero energy position of the energy scale was calibrated and checked with the known cross section curves of anions of  $\text{CCl}_4$  and  $\text{SF}_6$  [14].

As in previous studies, two homologous anion series are observed by electron attachment to the neutral oxygen cluster beam. Figure 2 (full line) shows the measured relative attachment cross section function for the production of  $O_2^-$  and  $(O_2)_2^-$  in the low energy regime produced via reaction



Measured cross sections exhibit the same characteristic behavior for all of these  $(O_2)_m^-$  ions, i.e., the cross section is largest at about zero energy and then strongly decreases with increasing energy. Moreover, the decreas-

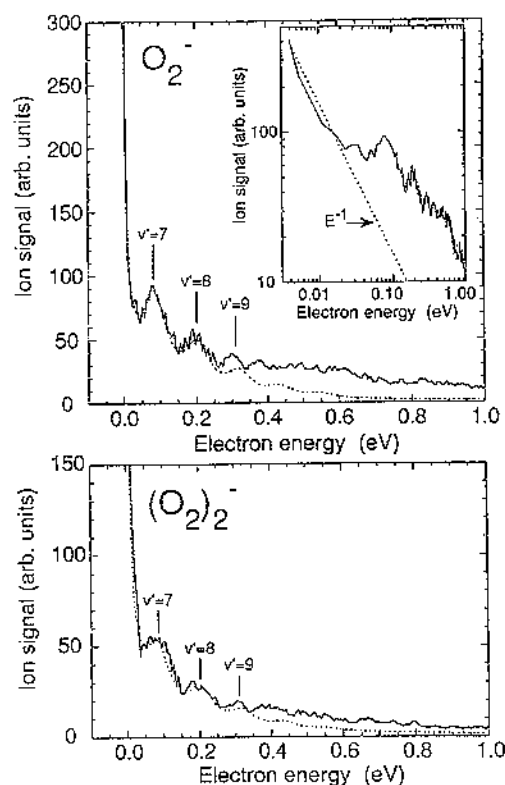


FIG. 2. Measured  $O_2^-$  (full line, upper panel) and  $(O_2)_2^-$  (full line, lower panel) anion signal produced by electron attachment to a  $(O_2)_n$  cluster beam as a function of corrected electron energy (electron current: 30 nA; energy resolution: 30 meV FWHM; guiding magnetic field: 50 G; ion extraction field: 100 meV/cm; stagnation pressure: 4.7 bars; stagnation temperature:  $-138^\circ\text{C}$ ). Also shown (broken line) is the calculated cross section behavior (see text). Inset: Measured  $O_2^-$  ion current versus corrected electron energy on a log-log scale. Dashed line indicates the  $E^{-1}$  dependence predicted by  $s$ -wave scattering theory.

ing cross section is structured by additional peaks whose maxima appear to lie (within the experimental error bar of  $\pm 10$  meV) in all cases at the same energy, i.e., for the  $O_2^-$  ion shown in Fig. 2 the distance between the zero energy and the first additional peak is 82 meV, to the next peak 193 meV, and to the final peak still discernible at 299 eV, respectively. On average, the first additional peak lies at an electron energy of about 80 meV, whereas the average spacing between the next two peaks is approximately 113 meV and 109 meV, respectively. In the following, we will first discuss the nature of the first peak and then proceed to the interpretation of the structures.

The inset in Fig. 2 gives a log-log plot of the measured  $O_2^-$  ion current versus electron energy. It can be seen that the anion current decreases strongly with increasing energy before the appearance of the additional structures at approximately 30 meV. This strong decrease is compatible with the energy dependence predicted by quantum theory [17] for  $s$ -wave scattering (i.e., an  $E^{-1}$  dependence), and such a strong decrease has been

observed for several molecules in this low energy region [9,13]. Thus we conclude that the present observation indicates that *s*-wave electron capture is also a likely mechanism in the electron attachment to oxygen clusters. After the initial *s*-wave capture of the electron by the entire  $(\text{O}_2)_n$  cluster, subsequent inelastic scattering processes (energy losses to phonons) reduce the electron energy below the vacuum level and lead, via monomer evaporation, to the final reaction product observed, i.e.,  $\text{O}_2^-$  (and higher homologues). It is interesting to note that a theoretical description of electron capture to  $(\text{CO}_2)_n$  clusters [18] also gives a strong decrease with increasing energy in this very low energy region.

Peaks at higher electron energies are attributed to the attachment of an incoming electron to a single oxygen molecule within the target cluster via a direct Franck-Condon transition from the ground vibrational state  $v = 0$  to a vibrational excited state  $v'$  of the ensuing anions (see lower part of Fig. 1). Subsequent collisional stabilization [19] of this anion within the cluster environment to a vibrational state below  $v' = 4$  gives a stable  $\text{O}_2^-$ . The energy thus released leads to the evaporation of neutral oxygen molecules (the heat of condensation of  $\text{O}_2$  with 1.63 kcal/mole [20] being the order of magnitude in energy which can be disposed in a single evaporation step). Depending on the amount of energy released (which depends on the  $v'$  state reached, see below) and on the size of the neutral precursor, this may lead to the production of naked  $\text{O}_2^-$  ions or to higher homologues such as  $\text{O}_4^-$ ,  $\text{O}_6^-$ , etc.

Identification of the vibrational states populated in the anion can be done in two ways. Despite an absolute error margin of  $\pm 10$  meV in the energy position of the peaks, the relative error for the vibrational spacings determined is much smaller, amounting to about  $\pm 5$  meV. This gives a value of about 118 meV as an upper limit of the spacings which is certainly smaller than the known spacing between the  $v' = 4$  and  $v' = 5$  state of 125 meV [21]. From the table of the slowly decreasing spacings with increasing  $v'$  (given in Ref. [21] for the monomer), the peak present at 80 meV thus has to be either  $v' = 7$  (as indicated in Fig. 1) or a higher state, assuming similar spacings in the monomer and solvated anion.

A similar result is obtained from the calculation of the downward shift of the anion potential in the cluster environment due to polarization forces (see [22]). To this end, we assume that the excess electron is localized initially on a specific molecule within the cluster. This is a good approximation, because the cluster is only weakly bound by van der Waals forces, and the distance between the molecules is large. Thus delocalization of the excess electron only becomes important later, when strongly bound dimer or trimer anions are formed via intracluster reactions. The electric field of the negative charge then polarizes the other molecules of the cluster. The corresponding energy  $V_p$  has been calculated using

the model given in Ref. [23] and strongly depends on the position  $r$  of the molecular anion in the cluster, and on the size and the structure of the cluster. A constant temperature molecular dynamics calculation ( $T = 20$  K) yields the distributions  $f$  for  $V_p$ , which are shown for the three cluster sizes 10, 15, and 20 in Fig. 3 as a function of the adiabatic electron affinity (defined as the sum of the polarization energy  $V_p$  and the adiabatic electron affinity of the monomer).

Two important conclusion can be drawn from the results shown in Fig. 3. At a typical cluster temperature of 20 K there exists only a small range of possible polarization energies independent of the precursor sizes probed. Thus the shift induced by this polarization energy is well defined, and the value of 0.8 eV for the total adiabatic electron affinity (thereby assuming that the initial neutral precursor has an approximate size of 15 to 20 molecules, which is also compatible with the energy necessary to evaporate 14 of those molecules) is close to the value used for constructing the hypothetical potential curves shown in the lower part of Fig. 1. This leads to a situation where  $v' = 7$  is the first vibrational state accessible via a vertical Franck-Condon transition by electron attachment in accordance with the conclusion drawn above from a comparison between the measured and the known vibration spacings. Moreover, a further confirmation of this identification comes from a calculation where we have modeled the energy dependence of the attachment cross section (see broken line in Fig. 2), adding to the *s*-wave scattering component calculated contributions resulting from the respective Franck-Condon overlap

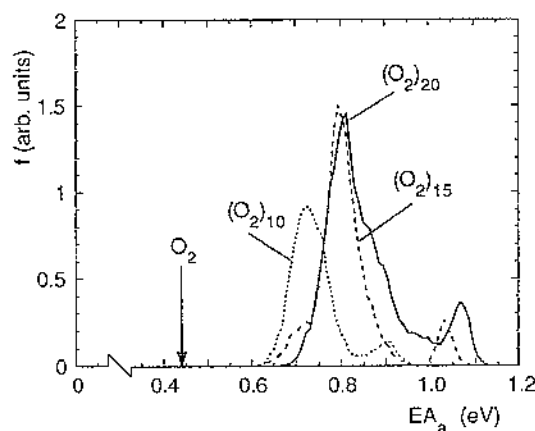


FIG. 3. Calculated distribution function  $f$  (for the various possible cluster structures and various positions of the solvated  $\text{O}_2^-$  ion in the cluster, respectively) of the adiabatic electron affinity  $EA_a$ , taking into account the polarization energy  $V_p$  in the nascent cluster anion for neutral precursor sizes of 10, 15, and 20 oxygen molecules at 20 K cluster temperature. The arrow designated  $\text{O}_2$  indicates the electron affinity of the single molecule. The first (major) peak around 0.8 eV is due to structures where the anion is assumed to reside at the surface of the cluster, and the second (minor) peak around 1 eV is due to anions at the center.

integrals. Note that the peaks in Fig. 2 for  $v' = 7, 8, 9$  have a slightly larger width than the peak in Fig. 3 at 0.8 eV. The excellent agreement between the experimental shape and the theoretical prediction (up to the fourth peak, see Fig. 2; the higher order transitions are possibly contaminated in the experiment by additional reaction channels above 0.4 eV, e.g., *p*-wave capture) not only confirms the vertical shift when going in Fig. 1 from the monomer to the cluster, but also the horizontal position of the hypothetical potential energy curve, i.e., using for the anion in the cluster case the same bond distance of  $1.34 \times 10^{-10}$  m as in the monomer case [4].

In conclusion, we report, for the first time, vibrationally resolved electron/cluster attachment spectra measured in a crossed beam arrangement under single collision conditions. This is possible using a high performance monochromator in conjunction with a cryostat cooled cluster source and a high efficiency detection system. The measured electron energy dependence demonstrates, on the one hand, that, at energies close to zero, the incoming electron is very likely captured by the entire cluster via *s*-wave scattering, whereas peaks at higher energy can be quantitatively ascribed to the vertical attachment of the incoming electron at one cluster molecule, thus leading to the Franck-Condon transition from the vibrational ground state of the neutral to the excited vibrational states in the anion with  $v' \geq 7$ .

This work was partially supported by the österreichischer Fonds zur Förderung der Wissenschaftlichen Forschung and the Bundesministerium für Wissenschaft, Forschung und Kunst, Wien, Austria

\*Permanent address: Katedra fyziky plazmy, Univerzita Komenského, Mlynska dolina F2, 84215 Bratislava, Slovakia.

†Permanent address: Institute of Physics and Meteorology, PMF Beograd, P.O. Box 550, 11001 Beograd, Yugoslavia.

- [1] G.E. Caledonia, *Chem. Rev.* **75**, 33 (1975); L.G. Christophorou, *Rad. Phys. Chem.* **12**, 19 (1978); T. Oster, A. Kühn, and E. Illenberger, *Int. J. Mass Spectrom. Ion Proc.* **89**, 1 (1989).
- [2] Y. Hatano and H. Shimamori, in *Electron and Ion Swarms*, edited by L.G. Christophorou (Pergamon, New York, 1981), p. 103.
- [3] F.C. Fehsenfeld and E.E. Ferguson, *Planetary Space Sci.* **15**, 701 (1968).
- [4] R.J. Celotta, R.A. Bennett, J.H. Hall, M.W. Siegel, and J. Levine, *Phys. Rev. A* **6**, 631 (1972).
- [5] D. Spence and G.J. Schulz, *Phys. Rev. A* **5**, 724 (1972).
- [6] D.L. McCorkle, L.G. Christophorou, and V.A. Anderson, *J. Phys. B* **5**, 1211 (1972).
- [7] M.J.W. Boness and G.J. Schulz, *Phys. Rev. A* **2**, 2182 (1970).
- [8] J.E. Land and W. Raith, *Phys. Rev. Lett.* **30**, 193 (1973).
- [9] L.G. Christophorou, D.L. McCorkle, and A.A. Christodoulidis, in *Electron-Molecule Interactions and Their Applications*, edited by L.G. Christophorou (Pergamon, New York, 1984) p. 477.
- [10] G.J. Schulz, *Revs. Mod. Phys.* **45**, 423 (1973).
- [11] T.D. Märk, K. Leiter, W. Ritter, and A. Stamatovic, *Phys. Rev. Lett.* **55**, 2559 (1985); G. Walder, D. Margreiter, C. Winkler, V. Grill, T. Rauth, P. Scheier, A. Stamatovic, Z. Herman, M. Foltin, and T.D. Märk, *Z. Phys. D* **20**, 201 (1991).
- [12] T. Jaffke, R. Hashemi, L.C. Christophorou, and E. Illenberger, *Z. Phys. D* **25**, 77 (1992); R. Hashemi and E. Illenberger, *Chem. Phys. Lett.* **187**, 623 (1991).
- [13] S. Matejcik, A. Kiendler, A. Stamatovic, and T.D. Märk, *Int. J. Mass Spectrom. Ion Proc.* **149/150**, 311 (1995).
- [14] S. Matejcik, Ph.D. thesis, University of Innsbruck, 1995 (unpublished).
- [15] S. Matejcik, P. Eichberger, B. Plunger, A. Kiendler, A. Stamatovic, and T.D. Märk, *Int. J. Mass Spectrom. Ion Proc.* **144**, L13 (1995).
- [16] M. Lezius, T. Rauth, V. Grill, M. Foltin, and T.D. Märk, *Z. Phys. D* **24**, 289 (1992).
- [17] N.F. Mott and H.S.W. Massey, *The Theory of Atomic Collisions* (Clarendon Press, Oxford, 1965).
- [18] M. Tsukada, N. Shima, S. Tsuneyuli, H. Kageshima, and T. Kondow, *J. Chem. Phys.* **87**, 3927 (1987).
- [19] M. Foltin, V. Grill, and T.D. Märk, *Chem. Phys. Lett.* **188**, 427 (1992); O. Ingolfsson and E. Illenberger, *Chem. Phys. Lett.* **241**, 180 (1995).
- [20] K. Hiraoka, *J. Chem. Phys.* **89**, 3190 (1988).
- [21] G.J. Schulz, in *Electron-Molecule Scattering*, edited by S.C. Brown (Wiley, New York, 1979), p. 43.
- [22] L. Sanche and M. Deschenes, *Phys. Rev. Lett.* **61**, 2096 (1988).
- [23] D.C. Conway, *J. Chem. Phys.* **52**, 2689 (1970).



Given the significant amount of variability, this new theory provides a plausible driving mechanism for the reversal of the magnetic poles of the sun as well as for the magnitude and duration of the solar activity level. Furthermore, it can lead to much better predictability of not only the solar maxima, but also of their duration and magnitude. In addition, this theory gives rise for a mechanism for the magnetic field of the planets to change and reverse.

The explanation is as follows: according to equation (1), the position of the planets in the solar system with respect to each other and with respect to the sun determine the flow of electrons along the diallel lines and along magnetic field lines. It is like having paths of conductivity and resistivity for the solar emissions as the planets move with respect to the spin axis of the sun and with respect to each other. Here, we have to account for both the tilt angle of the planets as well as their orbital planes as we look at conductivity and resistivity for emission electron paths. The sun is the source, the planets are the sinks and their parallel augmentation directly affects the effective conductivity -- hence the flow (quantity) of electrons.

As an illustrative example, the periods of the planets and their harmonic relationship to the period of the solar sunspot cycle are shown in the following table.

<b>Planets' Periods and Ratio to Solar Magnetic Cycle</b>			
<b>Planet</b>	<b>Period</b>		<b>Ratio</b>
Mercury	88	days	3:274
Venus	224.7	days	4:143
Earth	1.0	year	22
Mars	1.88	years	3:35
Jupiter	11.86	years	7:13
Saturn	29.46	years	4:3
Uranus	84.01	years	4:1
Neptune	164.8	years	15:2
Harmonic Relationship between Planets' Periods and Solar Magnetic Cycle			

In general terms, we see these integer harmonic relationships between the main planet periods and the solar magnetic period of 22 years. The inference is that 22 years is in a harmonic relationship with the periods of the planets. According to our new unified field theory the electron flow in the solar system along diallel, gravitational-field lines will be impacted directly by these harmonic relationships as the planets increase and decrease their susceptibility to electrons from the sun -- since it is the source. This will then cause a repeat in the direction of electron flow through the center of the sun with a 22 year period. The planets being nominally out of phase on the 11 year half cycle will induce a reversal of the magnetic field.

All of the gas-giant planets plus the earth have significant magnetic fields. Aurora have been observed on Jupiter and Saturn. These magnetic fields increase the electron receptivity of these planets significantly, and they are principal in their harmonic relationships with the solar magnetic cycle. Here the  $A_2$  term in equation (1) becomes very important as we consider energy flow (electrons especially) along parallel diallel gravitational-field lines as a pair of planets with significant magnetic fields comes into alignment with the sun.

Using the software developed by William Riley [Riley] for characterizing the performance of the clocks used in the Global Positioning System (GPS), all of the recorded sunspot activity data were analyzed to look for planetary resonances. See Figure 6. As one looks at the plot, one sees peaks and valleys for sigma -- the frequency stability. Sigma minimum values (valleys) can occur when J is equal to the period (1/frequency) of a periodic phenomena that is present in the data. The first major minimum corresponds to 10 times the orbit period of the Earth, 5 times the orbit period of Mars, and to the orbit period of Jupiter. The second minimum corresponds to the 22 year period of the sunspot cycle. The third minimum corresponds to the orbit period of Saturn. The J values are not long enough to detect the orbit periods of Uranus and Neptune. If one studies the stability data in detail, very slight minima occur at the orbit period J values for the Earth and Mars.

Since the periods,  $J_i$ , of the planets are well known, one can form the following equation as a model for the magnetic field conductance for the  $i^{\text{th}}$  planet:

$$C_i = A_i \cos(2Bt/T_i + B_i) *$$

\*" B" should read " $\pi$ "

All the planets except Mercury, Venus and Pluto seemed to have significant magnetic coefficients. See the web site for more detail [[www.allanstime.com](http://www.allanstime.com)]. According to equation (1) the value of  $B_i$  should correspond with north-magnetic pole solstice for a planet, in other words, when the north-magnetic pole is facing the sun to the greatest extent. This was tested for the Earth, Jupiter and Saturn. The average agreed to about 1 percent of a cycle with a standard deviation of 15 percent. Like the sun, the data give evidence that the magnetic poles of Jupiter and Saturn are also changing. It appears that Saturn's field has changed this century and Jupiter's is changing slowly. Currently, the magnetic field direction for Jupiter and Saturn are opposite that of the Earth, and Jupiter's is slowly increasing.

Because of the highly non-linear nature of the conductance causing the electron flow from the sun, frequency differences are also present in the data. It seems that the principle term in the sunspot cycle is due to the difference (or beat) frequency between the changing magnetic field of Jupiter and Jupiter's orbit frequency.

Again according to equation(1), the parallel portion given by the equation shows itself in a fundamental way as a pair of planets line up with the sun. This occurs frequently and adds significantly to the electron flow from the sun and hence in the model to the sunspot activity. For example, the big sunspot peak around 1960 is centered with the alignment of Jupiter and Neptune. Since Jupiter's magnetic field appears to be increasing, which is consistent with the two sets of Voyager data, the magnetic field of Neptune must be decreasing -- to explain the sunspot data observed.

A model was developed using the planetary data as an estimate of the driving mechanism for the sunspot data. The actual and the model of the sunspot data are shown in the figure for this century. The model is projected through the year 2,000. See Figure 7.

### **Alignment of the Planets, 5 May 2000**

There has been a lot of discussion about the coming nominal alignment of the planets on 5 May 2000. Classical gravitational theory predicts a small and relatively insignificant impact on earth tides and weather patterns from this alignment.

From this new unified field theory, the principal issue is the alignment of Jupiter and Saturn, which actually occurs about 13 June 2000. Numerous similar alignments have taken place during the 1900s. The 5 May alignment is as follows taking the line between the sun and Jupiter as zero degrees and measuring counter-clockwise from a north pole view: Mercury is +20, Venus +22, earth +192.5, and Mars is +340 degrees. The line between Jupiter and Saturn, which is the important one according to this new theory is -10 degrees on that date. The parallel part of equation(1) tells us that the closer the alignment the more significant the effect is on the conductivity of electrons from the sun and the resulting energy-density, so the important date is 13 June 2000.

Fortunately, since the Earth will be on the opposite side of the sun from Jupiter and Saturn, the principle conductivity path will then be away from us. If the earth were in that path, it would be party to this heavy electron flow and would be impacted quite significantly. But with the earth being on the opposite side, the earth will receive the secondary effect from the build up of the sunspot activity. That is to say, the 13 June alignment could significantly impact our ionosphere, which could affect communications and space probes.

In addition, the resulting excess electron flow around the date of 13 June 2000 along with the extra core heating of the Earth due to the accumulated effects of all the nuclear bomb testing activity integrated since the 1940s may cause an increase in the probability of earth quakes, volcanoes and increased weather activity. During this time the Aurora Borealis for the earth could become very large. This could also be true for Jupiter and Saturn.

- ■ - ■ - ■ - ■ - ■ - ■ - ■ - ■ -

[Return to Unified Field Theory index](#)

## See also:

- **Alignment of Planets and Magnetic Field-Sun Interactions** - Magnetic field interactions in planet alignments more significant than the gravity tugs.
- **Increased Solar Flare Activity and Planet Alignment Correlated**
- **New Theory of Gravity** - New gravity model by David W. Allan introduces an energy density component and diallel, gravitational-field lines as part of new Unified Field Theory.

Page Created May 5, 2000

Last updated